

# Evaluation of a New MRI-Based Classification of Graft Status After Superior Capsule Reconstruction

Jun-Bum Lee,\* MD, Erica Kholinne,<sup>†</sup> MD, PhD, Ji Woong Yeom,\* MD, Sang-Pil So,\* MD, Hui Ben,<sup>‡</sup> MD, Hood Alsaqri,\* MD, Kyoung-Hwan Koh,\* MD, PhD, and In-Ho Jeon,\*<sup>§</sup> MD, PhD

*Investigation performed at the Department of Orthopaedic Surgery, Asan Medical Center, University of Ulsan College of Medicine, Seoul, Republic of Korea*

**Background:** A classification system for the graft state after superior capsule reconstruction (SCR) using magnetic resonance imaging (MRI) has not been described previously.

**Purpose:** To introduce a new, MRI-based classification system for graft integrity after SCR and to evaluate the system according to postoperative outcomes.

**Study Design:** Cohort study (diagnosis); Level of evidence, 3.

**Method:** Included were 62 consecutive patients who underwent SCR using autologous fascia lata graft between January 2013 and April 2021. Postoperative outcomes were assessed (American Shoulder and Elbow Surgeons [ASES] score, Constant score, pain visual analog scale [pVAS], range of motion [ROM], acromiohumeral distance [AHD], Hamada grade). Graft status was classified by 2 orthopaedic surgeons on postoperative MRI in accordance with the signal intensity and the presence or extent of the tear, as follows: type 1 (hypointense signal without tear), type 2 (hyperintense signal without tear), type 3 (partial-thickness tear), type 4 (full-thickness tear with partial continuity), and type 5 (full-thickness tear with complete discontinuity). Intra- and interobserver agreement were assessed using Cohen kappa. The correlation between postoperative outcomes (ASES score, Constant score, pVAS, ROM, AHD, and Hamada grade) and the SCR graft classification system was assessed with the Pearson correlation coefficient, and the outcomes were compared according to classification type.

**Results:** Patients were classified according to the new system as follows: type 1 (n = 15), type 2 (n = 20), type 3 (n = 7), type 4 (n = 8), and type 5 (n = 12). There was excellent interobserver agreement ( $\kappa = 0.819$ ) and intraobserver agreement ( $\kappa = 0.937$  and  $0.919$ ). The classification system showed a moderate to high correlation with the ASES score ( $r = -0.451$ ;  $P = .001$ ), pVAS ( $r = 0.359$ ;  $P = .005$ ), AHD ( $r = -0.642$ ;  $P < .001$ ), and Hamada grade ( $r = 0.414$ ;  $P < .001$ ). Patients classified as having types 1 and 2 showed better outcomes in terms of ASES score, pVAS, ROM, and AHD compared with type 5 patients ( $P \leq .021$  for all).

**Conclusion:** The new classification system was highly reproducible and showed clinical utility for both radiological and clinical evaluation after SCR.

**Keywords:** auto fascia lata; classification system; clinical outcome; graft; MRI; superior capsule reconstruction

Studies regarding superior capsule reconstruction (SCR) as an alternative treatment for massive irreparable rotator cuff tears have been increasing.<sup>2,13,17,21,39</sup> SCR, which utilizes the autologous fascia lata as a humeral head depressor, was introduced by Mihata et al in 2012.<sup>27,29</sup> SCR reinforces superior static stability and prevents superior migration of the humeral head caused by the massive rotator cuff tear. Many studies have reported favorable clinical outcomes of SCR,<sup>2,21,25-27,39,40</sup> and graft healing is an important factor in this regard.<sup>15,16,25,40</sup>

The established Sugaya classification<sup>36</sup> uses postoperative magnetic resonance imaging (MRI) to evaluate the quality of tendon healing using 5 grades after rotator cuff repair surgery and is useful for assessing the condition of the tendons.<sup>24,32,41</sup> However, healing from an SCR using autologous fascia lata is referred to as “graft healing,” which is not the same as the “tendon healing” that occurs after rotator cuff repair.

The primary aim of this study was to classify patients after SCR based on graft integrity status using an MRI-based system similar to the Sugaya classification system for rotator cuff tendon healing. The secondary aim was to evaluate clinical outcomes according to this classification. We postulated that comparisons of clinical outcomes in

The Orthopaedic Journal of Sports Medicine, 11(9), 23259671231193315

DOI: 10.1177/23259671231193315

© The Author(s) 2023

This open-access article is published and distributed under the Creative Commons Attribution - NonCommercial - No Derivatives License (<https://creativecommons.org/licenses/by-nc-nd/4.0/>), which permits the noncommercial use, distribution, and reproduction of the article in any medium, provided the original author and source are credited. You may not alter, transform, or build upon this article without the permission of the Author(s). For article reuse guidelines, please visit SAGE's website at <http://www.sagepub.com/journals-permissions>.

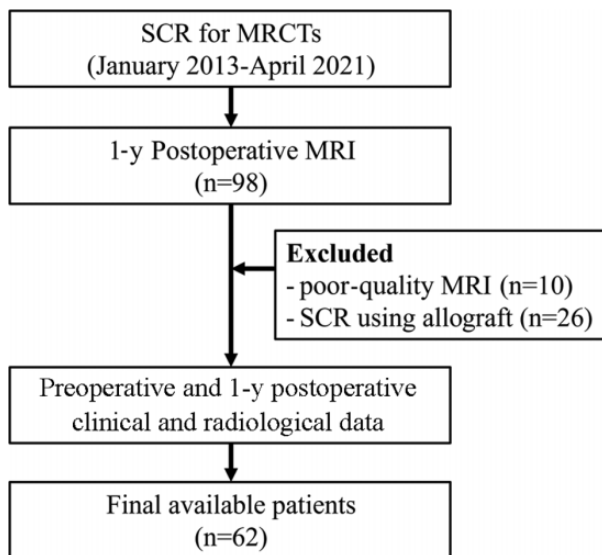


**Figure 1.** Study flow diagram. MRCT, massive rotator cuff tear; MRI, magnetic resonance imaging; SCR, superior capsule reconstruction.

accordance with the new SCR graft classification system would be applicable in clinical practice.

## METHODS

The protocol for this study was approved by our institutional review board. Between January 2013 and April 2021, a total of 131 consecutive patients underwent SCR by a single surgeon (I.H.J.) at our hospital. All patients in this population who underwent postoperative MRI after 1 year were identified ( $n = 98$ ). Among them, we excluded patients with a poor-quality MRI that was not suitable for graft evaluation ( $n = 10$ ) and those who received SCR using an allograft ( $n = 26$ ). Ultimately, a total of 62 patients were included in the analyses (Figure 1).

### SCR Surgery

After an irreparable rotator cuff tear was diagnosed via a diagnostic arthroscopy, we performed acromioplasty to reduce the friction between the subacromial undersurface and the graft. Subscapularis (SSC) repair was also performed in cases with concomitant SSC tears. The defect was

measured in the medial-lateral and anterior-posterior directions.

The fascia lata was harvested from the ipsilateral thigh and prepared as a double-folded 2-layer graft. A running suture with Ethibond (Ethicon) 2-0 in the graft margin was used. A graft of at least 6 mm in thickness was obtained in the final preparation, which was recorded in the operation record. After debridement of the superior margin of the glenoid, 2 or 3 suture anchors (1.7-mm Suture fix Anchor; Smith & Nephew) were inserted from the 10-o'clock to 2-o'clock position according to the defect size. A sliding locking knot suture was used on each anchor. A double-row suture bridge method was used for humeral side fixation. Two threaded anchors (4.5-mm Heali-coil; Smith & Nephew) were inserted anteriorly and posteriorly to the medial row of the footprint, respectively, and the graft was fixed with a mattress suture. Remnant rotator cuff tissue or subacromial bursa were sutured using remaining strings from the medial row anchors and fixed with 2 knotless anchors (4.5-mm; Footprint Anchor; Smith & Nephew) inserted into the lateral row of the footprint. All graft fixations were performed in a 30° shoulder abduction and neutral rotation position. (Figure 2). In 38 of 62 patients (61.29%), mesh was implemented between the grafts to enhance stiffness.<sup>16</sup>

### Postoperative Rehabilitation

Immobilization for 6 to 8 weeks with an abduction brace was performed in all patients. After immobilization, a passive range of motion (ROM) exercise program was started. After a full ROM was achieved, strengthening exercise programs including elastic band exercises and periscapular muscle strengthening exercises were commenced. Patients were recommended to return to daily activities within a tolerable range at 3 months after surgery, while leisure sports activities were allowed 1 year after surgery.

### Patient Data, Radiological Assessment, and Shoulder MRI

Patient information (age, sex, underlying disease, and history of previous surgeries) was collected through a review of electronic medical records. Clinical outcomes (ROM, pain visual analog scale [pVAS], American Shoulder and Elbow Surgeons [ASES] score, and Constant score) measured preoperatively and at 1 year postoperatively were retrieved from the medical records.

The Hamada classification system was used to evaluate the stage of cuff tear arthropathy on plain radiographs taken preoperatively and 1 year postoperatively. The acromiohumeral distance (AHD) was measured using

<sup>§</sup>Address correspondence to In-Ho Jeon, MD, PhD, Department of Orthopaedic Surgery, Asan Medical Center, University of Ulsan College of Medicine, 88 Olympic-ro 43-gil, Songpa-gu, Seoul 05535, Republic of Korea (email: jeonchoi@gmail.com).

\*Department of Orthopaedic Surgery, Asan Medical Center, University of Ulsan College of Medicine, Seoul, Republic of Korea.

<sup>†</sup>Department of Orthopedic Surgery, St Carolus Hospital, Faculty of Medicine, Universitas Trisakti, Jakarta, Indonesia.

<sup>‡</sup>Asan Institute for Life Sciences, Asan Medical Center, University of Ulsan College of Medicine, Seoul, Republic of Korea.

Final revision submitted April 7, 2023; accepted May 3, 2023.

The authors have declared that there are no conflicts of interest in the authorship and publication of this contribution. AOSSM checks author disclosures against the Open Payments Database (OPD). AOSSM has not conducted an independent investigation on the OPD and disclaims any liability or responsibility relating thereto.

Ethical approval for this study was obtained from Asan Medical Center (No. 2022-0996).

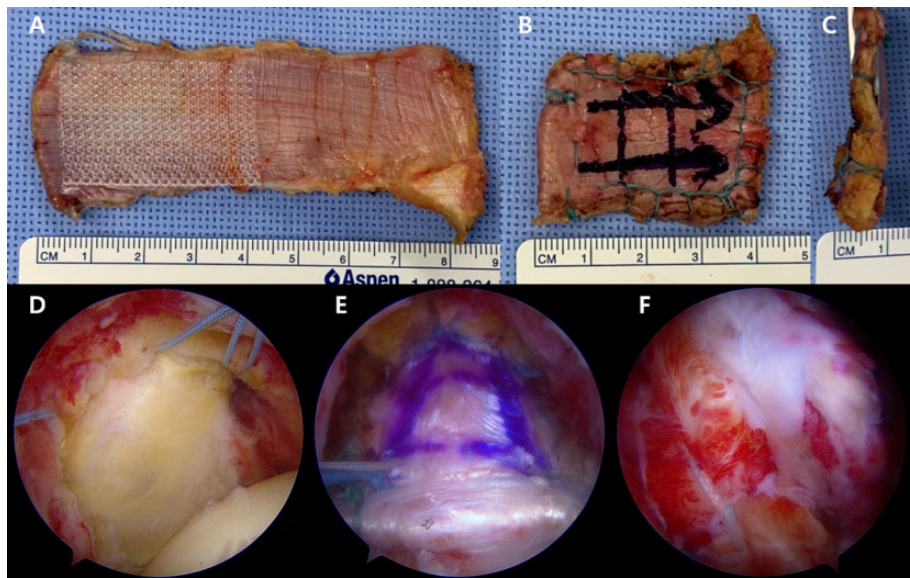


**Figure 2.** Graft preparation and superior capsule reconstruction procedure. (A) Polypropylene mesh augmentation. (B) Marginal running suturing. (C) The mean thickness of the graft was at least 6 mm. (D) Suture anchors were inserted in the 10-o'clock to 2-o'clock direction of the superior surface of the glenoid. (E) After fixation of the graft at each side of the glenoid and the humerus. (F) Remnant tissues including rotator cuff tendon and bursa tissues were repaired on the graft (over the top technique) and fixed.

preoperative and 1-year postoperative plain radiographs obtained with the shoulder in a neutral position.

Pre- and postoperative shoulder MRIs were performed using a 3-T scanner (Ingenia; Philips). The following parameters were used on the scanner: axial and coronal T2 fat saturation (repetition time [TR] = 4700 ms; echo time [TE] = 65 ms), coronal T1 (TR = 640 ms; TE = 21 ms), and coronal and sagittal T2 (TR = 2880 ms; TE = 80 ms). Weighted images were acquired. The slice thickness was 2 mm with an interslice gap of 0.5 mm (field of view, 150 mm; image matrix, 512 × 512). The imaging data were jointly reviewed and evaluated by 2 orthopaedic surgeons (J.-B.L. and J.W.Y.). To evaluate preoperative characteristics of the shoulder pathology, fatty infiltration (FI) of the rotator cuff muscle and tendon retraction were assessed using preoperative MRI. The preoperative FI of the rotator cuff muscle was assessed using the Goutallier classification: grade 0 for normal muscle, grade 1 for muscle with fatty streaks, grade 2 for muscle with greater FI, grade 3 for muscle with equal FI, and grade 4 for muscle with lesser FI.<sup>7,10,35</sup> The degree of tendon retraction was evaluated using the Patte classification on coronal and axial views of the shoulder.<sup>16,33</sup> grade 1, in which the tear stump of the tendon is retracted and located before the lateral articular margin; grade 2, in which the stump is at the level of the humeral head; grade 3, in which the stump is at the glenoid level; and grade 4, in which the stump is located medially to the glenoid level.<sup>33</sup>

### MRI Assessment of Graft Integrity

Postoperative MRI was performed at 1 year postoperatively to evaluate the graft integrity. We identified the graft tissue between the inserted anchors to reduce the possibility of misreading torn graft when the MRI cut

direction was not parallel to the graft direction. To determine the integrity of the graft, several consecutive cuts of the images were checked in the coronal and sagittal views (Figure 3).

The thickness of the graft was checked in both the sagittal and coronal views and was categorized as normal, partial tear, or a complete tear according to the depth of the tear in the graft. The intrasubstance hypersignal intensity of the graft was determined when there was only a signal change without graft tear. The proposed graft classifications after SCR were as follows (Figure 4): type 1, graft with no tear and with homogeneously low intensity on each image; type 2, graft with no tear with intrasubstance hypersignal intensity; type 3, graft with a partial-thickness tear; type 4, graft with a full-thickness tear but with partial integrity; and type 5, graft with a full-thickness tear and complete discontinuity.

### Intra- and Interobserver Reliability of SCR Graft Classifications

Two orthopaedic shoulder specialists (J.-B.L. and J.W.Y.) participated in the reproducibility assessment of the new classification system for graft healing after SCR. Each observer independently classified the graft status twice in accordance with this new system, with an interval of at least 4 weeks between assessments.

### Clinical and Radiological Outcomes

An independent examiner (J.W.Y) who was not involved in any of the surgeries conducted the clinical assessments of the study patients. The preoperative and 1-year postoperative clinical outcomes (ASES score, Constant score, pVAS,



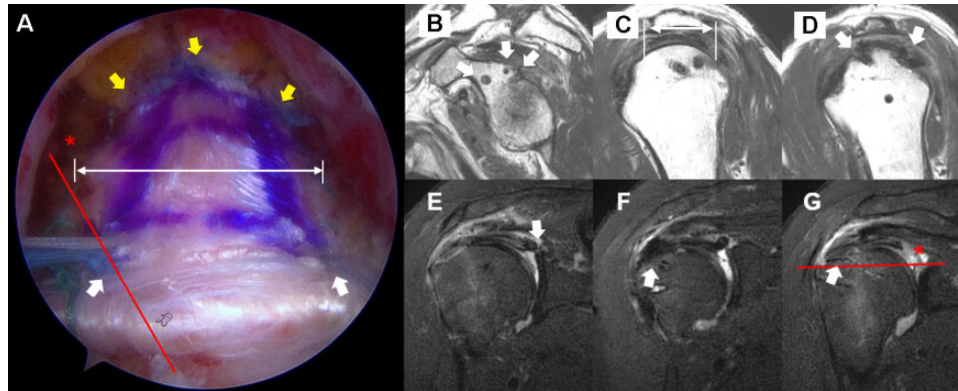


**Figure 3.** Comparisons between (A) arthroscopic view and (B-G) postoperative MRI. (A) Arthroscopic view from a standard lateral portal. The autologous fascia lata graft was placed between the glenoid and humerus and fixed with anchors at each side. The yellow arrows indicate the locations of the glenoid anchors, the large white arrows indicate the locations of the humerus anchor, the horizontal white line represents the width of the graft, the red line represents the virtual line of the coronal section MRI, and the red asterisk represents a pseudotear shown in (G). (B-D) T2-weighted sagittal view postoperative MRI scans. (B) Anchors were inserted into the glenoid (white arrows). (C) Midpoint of the graft. The horizontal white line represents the graft width. (D) Anchors were inserted into the humerus (white arrows), and the graft was placed between the anchors. (E-G) T2-weighted fat-suppressed coronal view postoperative MRI scans. The graft was placed between the anchors (white arrows). (G) A graft tear-like finding (red asterisk), but a pseudolesion due to the direction of MRI acquisition (red line), which was not parallel to the graft. MRI, magnetic resonance imaging.

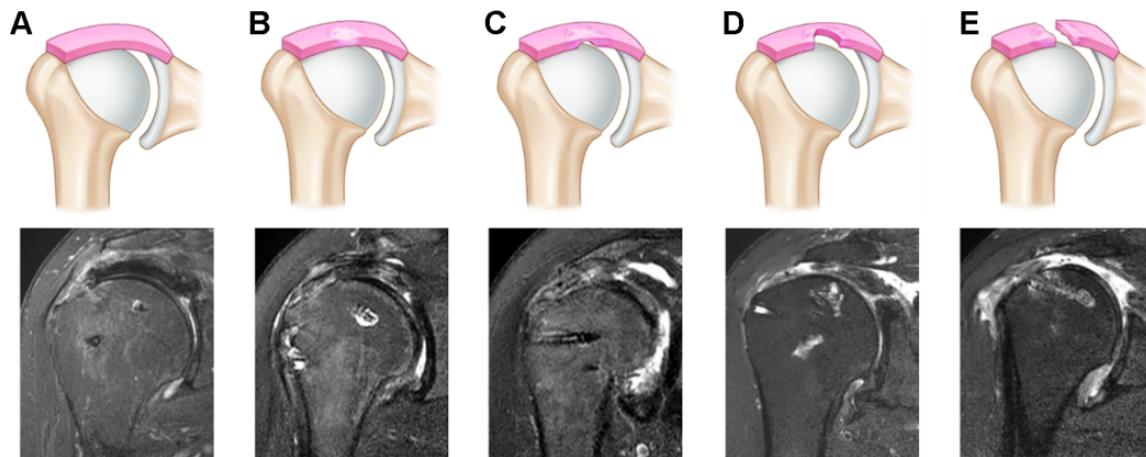


**Figure 4.** Schematic images and postoperative MRIs of SCR grafts classified into 5 categories. (A) Type 1, graft with no tear and with homogeneously low intensity on each image. (B) Type 2, graft with no tear with intrasubstance hypersignal intensity. (C) Type 3, graft with a partial-thickness tear. (D) Type 4, graft with a full-thickness tear but with partial integrity. (E) Type 5, graft with a full-thickness tear and complete discontinuity. MRI, magnetic resonance images; SCR, superior capsule reconstruction.

and ROM) and radiological (AHD and Hamada classification<sup>12</sup>) outcomes were compared according to SCR graft type under the new classification. Due to the small number of included study patients, types 1 and 2 were combined into group A (without tear), types 3 and 4 were combined into group B (tear but with continuity), and type 5 was regarded as group C (without continuity) for statistical analysis.

### Statistical Analysis

Quantitative data are described as mean  $\pm$  standard deviation and qualitative data as number and percentage. Data sets for measured parameters were compared using the

Mann-Whitney *U* test for continuous data and the Fisher exact test for categorical data. For intergroup comparisons (groups A versus group B versus group C), analysis of variance with Tukey post hoc test was used. The intra- and interobserver reliability of the MRI assessments were calculated using the Cohen kappa coefficient ( $\kappa$ ),<sup>4</sup> with  $\kappa$  values interpreted as described by Landis and Koch<sup>18</sup>:  $<0$  (no agreement), 0 to 0.20 (slight agreement), 0.21 to 0.40 (fair agreement), 0.41 to 0.60 (moderate agreement), 0.61 to 0.80 (substantial agreement), and 0.81 to 1.00 (almost perfect agreement). The Pearson correlation coefficient (*r*) was used to evaluate the correlations between the clinical outcomes and the new SCR classification

TABLE 1  
Demographic, Clinical, and Radiological Characteristics of the Study Patients (N = 62)<sup>a</sup>

Demographic/Clinical Parameters	Value	Radiological Parameters	Value
Age, y	65.2 ± 8.5	Goutallier grade, 0/1/2/3/4	
Sex, male/female	21/41	Supraspinatus	1/7/40/11/3
Affected shoulder, right/left	48/14	Infraspinatus	2/16/24/15/5
Hypertension	28	Teres minor	36/25/0/0/1
Diabetes mellitus	10	Subscapularis	4/40/5/3/10
Prior shoulder operation	3	Patte grade	
Graft type, FL/FL with mesh	24/38	1 (greater tuberosity)	0
Follow-up duration, mo	28.5 ± 17.7	2 (humeral head exposure)	6
ASES score	49.3 ± 17.0	3 (glenoid)	48
Constant score	52.5 ± 12.5	4 (medial to glenoid)	8
pVAS score	4.7 ± 2.0	Hamada grade	
Active shoulder ROM, deg		1	22
Forward flexion	144.7 ± 38.2	2	33
External rotation	38.0 ± 21.6	3	4
		4a	3
		4b	0
		5	0
		AHD, mm	5.06 ± 2.11

<sup>a</sup>Data are shown as mean ± SD or n. AHD, acromiohumeral distance; ASES, American Shoulder and Elbow Surgeons; FL, fascia lata; pVAS, pain visual analog scale; ROM, range of motion.

system, in which *r* values <0.3 were considered low, 0.3 to 0.6 moderate, and >0.6 high. The significance level for all comparisons was set at *P* < .05. All descriptive and analytic analyses were conducted using SPSS version 21.0 (IBM Corp).

## RESULTS

### Patients

Among the 62 study patients (mean age, 65.2 ± 8.5 years), 21 (33.9%) were men. A concomitant SSC repair was performed in 9 (14.5%) patients. In most of the patients, the tear margin was retracted to glenoid level or more retracted medially (Patte grade 3 in 48 [77.4%] and grade 4 in 8 [12.9%]). Preoperative mean AHD was 5.06 ± 2.11 mm. The mean follow-up duration was 28.5 ± 17.7 months. Table 1 lists the patient demographics and preoperative clinical and radiological findings.

### SCR Graft Classifications and Intra- and Interobserver Agreement

According to the new SCR classification of the postoperative graft status, 15 patients were classified as type 1 (24.2%), 20 as type 2 (32.3%), 7 as type 3 (11.3%), 8 as type 4 (12.9%), and 12 as type 5 (19.4%). The intraobserver agreement among the assessments was almost perfect, with a mean  $\kappa$  coefficient of 0.937 and 0.919 in each observer. The interobserver agreement was almost perfect, with a mean coefficient of 0.819.

### Clinical and Radiological Outcomes According to SCR Graft Type

After surgery, patients in groups A, B, and C showed significant increases in their ASES (*P* < .001, *P* < .001, and *P* = .003, respectively) and pVAS (*P* < .001, *P* < .001, and *P* = .014, respectively) values compared with the preoperative levels. The Constant score was significantly elevated only in groups A and B (*P* < .001 for both). Improvement in forward flexion (FF) after SCR was only noted in group A (*P* = .016). External rotation showed no significant difference among the 3 groups. AHD was increased significantly in groups A and B (*P* < .001 and *P* = .004, respectively).

Postoperative ASES was significantly higher in group A (82.5 ± 7.4) than in group C (69.9 ± 10.8; *P* < .001). Postoperative pVAS was significantly lower in group A (1.19 ± 0.78) than in group C (2.08 ± 0.67; *P* = .021). Postoperative AHD was the highest in group A (*P* < .001). In terms of postoperative Hamada classification, group A showed a higher degree of improvement than group B (*P* = .030). Group C showed no improvement after SCR and there was 1 patient who showed progression in cuff tear arthropathy (Table 2).

### Correlation of SCR Classification System With Clinical/Radiological Outcomes

The new SCR graft classification system showed a moderate to high degree of correlation with ASES (*r* = -0.451; *P* = .001), pVAS (*r* = 0.359; *P* = .005), ROM FF (*r* = -0.496; *P* < .001), AHD (*r* = -0.642; *P* < .001), and Hamada classification (*r* = 0.414; *P* < .001) (Table 3).

TABLE 2  
Clinical and Radiological Outcomes According to SCR Graft Type<sup>a</sup>

	Group A (n = 35)	Group B (n = 15)	Group C (n = 12)	ANOVA		
				F	P <sup>b</sup>	Post Hoc
Clinical Outcomes						
ASES score						
Preop	49.40 ± 16.43	47.20 ± 17.69	54.58 ± 12.59	0.734	.484	NA
Postop	82.48 ± 7.42	80.75 ± 6.44	69.90 ± 10.82	9.411	<b>&lt;.001</b>	A = B > C
P <sup>c</sup>	<b>&lt;.001</b>	<b>&lt;.001</b>	<b>.003</b>			
Constant score						
Preop	51.51 ± 14.99	52.33 ± 8.73	55.33 ± 8.19	0.408	.667	NA
Postop	61.94 ± 5.18	62.84 ± 4.33	61.25 ± 7.43	0.262	.771	NA
P <sup>c</sup>	<b>&lt;.001</b>	<b>&lt;.001</b>	.063			
pVAS score						
Preop	4.88 ± 1.79	4.87 ± 2.39	4.08 ± 2.11	0.761	.472	NA
Postop	1.19 ± 0.78	1.6 ± 1.35	2.08 ± 0.67	4.150	<b>.021</b>	A > B = C
P <sup>c</sup>	<b>&lt;.001</b>	<b>&lt;.001</b>	<b>.014</b>			
ROM: FF						
Preop	142.94 ± 38.20	151.66 ± 29.74	152.91 ± 22.41	0.574	.567	NA
Postop	160.56 ± 8.70	155.36 ± 13.65	141.67 ± 18.90	8.879	<b>.001</b>	A = B > C
P <sup>c</sup>	<b>.016</b>	.601	.186			
ROM: ER						
Preop	40.45 ± 20.32	33.66 ± 20.04	42.91 ± 23.30	0.777	.464	NA
Postop	42.50 ± 15.91	40.00 ± 12.61	39.17 ± 17.30	0.248	.781	NA
P <sup>c</sup>	.348	.830	.351			
Radiological Outcomes						
AHD						
Preop	5.53 ± 2.14	4.61 ± 2.09	4.24 ± 1.81	2.204	.119	NA
Postop	7.33 ± 1.62	6.14 ± 1.90	4.52 ± 2.45	10.498	<b>&lt;.001</b>	A > B > C
P <sup>c</sup>	<b>&lt;.001</b>	<b>.004</b>	.732			
Hamada grade						
Preop, 1/2/3/4a/4b/5	13/19/3/0/0/0	3/11/1/0/0/0	3/7/2/0/0/0			
Postop, 1/2/3/4a/4b/5	32/3/0/0/0/0	6/9/0/0/0/0	3/7/1/0/0/1			
Improved	22	4	0		<b>.030<sup>d</sup></b>	
No change	13	11	11			
Worsened	0	0	1			

<sup>a</sup>Data are shown as mean ± SD or n. Boldface P values indicate statistically significant difference between groups compared as indicated (P < .05). AHD, acromiohumeral distance; ANOVA, analysis of variance; ASES, American Shoulder and Elbow Surgeons; ER, external rotation; FF, forward flexion; NA, not applicable; Preop, preoperative; Postop, postoperative; pVAS, pain visual analog scale; ROM, range of motion; SCR, superior capsule reconstruction. Group A = types 1 and 2 (without tear); Group B = types 3 and 4 (tear but with continuity); group C = type 5 (tear without continuity).

<sup>b</sup>Comparison among groups A, B, and C

<sup>c</sup>Comparison between preoperative and postoperative data.

<sup>d</sup>Chi-square analysis between groups A and B.

## DISCUSSION

Our SCR graft classification method showed almost perfect inter- and intraobserver reliability. Furthermore, this classification system showed moderate to high correlations with clinical (ASES and pVAS) and radiological (AHD and Hamada classification) outcomes. Type 5 classification in this system, which denotes a complete discontinuity of the graft, was significantly associated with poor clinical and radiological outcomes that were indicative of a failed SCR.

In the histological evaluation of SCR grafts, second-look arthroscopy and biopsy graft specimens are considered to be the gold standard; however, they are invasive and thus

not ideal for clinical follow-up.<sup>38</sup> Graft healing in the orthopaedic field is therefore mostly evaluated using MRI.<sup>9,11,22,34,37,42,43</sup> A detailed description of the graft status using MRI is important to distinguish whether the graft is healing or if a pathologic condition (eg, partial tear, total rupture) has emerged. Our new classification for the graft status after SCR uses 5 different grading scores. This system will therefore help orthopaedic surgeons or radiologists to describe the graft state in clinical practice. It will also have utility in describing graft changes in future studies.

In our study patients, image analysis was performed using an MRI reading protocol that clearly defined the

TABLE 3  
Correlation between SCR Classification System and  
Clinical/Radiological Outcomes<sup>a</sup>

	<i>r</i>	<i>P</i>
ASES score	-0.451	<b>.001</b>
Constant score	0.028	.84
pVAS score	0.359	<b>.005</b>
ROM: FF	-0.496	<b>&lt;.001</b>
ROM: ER	-0.131	.32
Abduction strength	0.058	.67
ER strength	-0.047	.73
IR strength	-0.019	.89
AHD	-0.642	<b>&lt;.001</b>
Hamada classification	0.414	<b>&lt;.001</b>

<sup>a</sup>Boldface *P* values indicate statistical significance ( $P < .05$ ). AHD, acromiohumeral distance; ASES, American Shoulder and Elbow Surgeons; ER, external rotation; FF, forward flexion; IR, internal rotation; pVAS, pain visual analog scale; ROM, range of motion; SCR, superior capsule reconstruction.

location and graft status with high reproducibility. The distinction between the graft and the surrounding tissue is an important factor in accurately determining the graft state on an MRI scan.<sup>16,20</sup> In some cases, distinguishing the graft from the surrounding tissue is difficult due to graft remodeling. In addition, if the direction of the graft and that of the MRI are not parallel, the possibility of misdiagnosing a graft tear should also be considered. Importantly, our imaging analysis with an MRI reading protocol showed almost perfect intra- and interobserver agreements.

The SCR graft classifications from our new system showed a moderate correlation with the clinical outcomes. Previous studies have reported that graft healing is the key to achieving favorable outcomes after SCR regardless of the graft materials used.<sup>5,25,26</sup> Pain from subacromial impingement, muscle weakness, and restricted active shoulder ROM are common symptoms of irreparable rotator cuff tear.<sup>6,8,23,31</sup> Defects in the superior capsule and posterosuperior rotator cuff tendons cause the loss of superior stability.<sup>1,14,28,29</sup> More severe symptoms may be caused by loss of stability of the glenohumeral joint.<sup>3</sup> In our present study, the graft healing group showed better clinical outcomes in terms of the ASES and pVAS values.

Our SCR classification system showed a moderate to high correlation with the AHD and Hamada classifications. Mihata and colleagues have reported that a healed graft provides superior stability and leads to significant increases in AHD.<sup>27</sup> In cases of failed graft healing, another study reported that a loss of superior stability leads to humeral head superior migration and subsequent progression of cuff tear arthropathy.<sup>25</sup> In our present study, the SCR graft classification showed significant correlations with AHD ( $r = -0.642$ ;  $P < .001$ ) and with the Hamada classification ( $r = 0.414$ ;  $P < .001$ ), suggesting that graft healing improves AHD and Hamada classification. However, Denard et al reported that preoperatively severely decreased AHD and advanced Hamada grade could be

correlated with postoperative graft failure.<sup>5</sup> The causal relationship between AHD and postoperative graft healing is thus still unclear, and further research is needed to investigate this.

In this present study, group A (without tear) was associated with the best clinical outcomes, followed by group B (tear with graft continuity) with intermediate clinical outcomes. Group C (tear with graft discontinuity) patients had relatively poor clinical outcomes. In previous MRI-based studies, comparative analyses were conducted in populations with graft tears and those with graft healing.<sup>19,20,25,27,40</sup> It is notable that, in relation to the postoperative graft status of the autologous fascia lata, the spectrum varies from no tear with hypointense signal to a full-thickness tear with complete discontinuity. To the best of the authors' knowledge, there has been no consensus or detailed descriptions regarding the definition of graft failure. In our current investigation of the association between clinical results and different graft types, the clinical outcomes (ASES, pVAS) and radiological outcomes (AHD and Hamada grade) were the best among patients with a type 1 graft status and the worst among patients with a type 5 graft status, whereas types 2, 3, and 4 did not show significant differences with type 1. Considering these results, type 5 (complete discontinuity) could be considered to indicate a failure of the SCR, both clinically and radiologically.

A previous study on graft classifications was conducted on patients in whom SCR was performed using alloderm.<sup>30</sup> In that report, the authors also used 5 categories to stratify the graft condition according to the presence and location of the tear as follows: intact, tear from the glenoid, midsubstance tear, tear from the tuberosity, and absent graft. However, there was no further description of the graft state in that study, which limited its capacity to explain and understand the changes that occurred due to autograft remodeling. Therefore, the classification system for SCR using alloderm may lead to some limitations in studies on SCR using autografts.

## Limitations

One limitation of our study was the small number of cases with impaired integrity of the graft. The numbers of patients with each designated graft state, especially types 3, 4, and 5, were too small for detailed analyses. Future studies with a larger sample size are necessary to perform analysis with the 5 subgroups of the classification. Another limitation of our study was the relatively short follow-up duration, which hindered us from analyzing the association of the proposed classification with long-term clinical outcomes. Future studies with a larger sample size and longer follow-up durations are needed to confirm the usefulness and suitability of our proposed grading system. Lastly, as all cases were treated with SCR using autologous fascia lata, there is a lack of evidence for the generalizability of this classification system to other graft types.

## CONCLUSION

The new SCR graft classification system introduced in this study was highly reproducible and showed clinical utility for both radiological and clinical evaluation following SCR. This system may support future studies regarding SCR with a consistent report of MRI-based outcomes.

## REFERENCES

- Adams CR, DeMartino AM, Rego G, Denard PJ, Burkhart SS. The rotator cuff and the superior capsule: why we need both. *Arthroscopy*. 2016;32(12):2628-2637.
- Altintas B, Scheidt M, Kremser V, et al. Superior capsule reconstruction for irreparable massive rotator cuff tears: does it make sense? A systematic review of early clinical evidence. *Am J Sports Med*. 2020;48(13):3365-3375.
- Chung SW, Kim JY, Kim MH, Kim SH, Oh JH. Arthroscopic repair of massive rotator cuff tears: outcome and analysis of factors associated with healing failure or poor postoperative function. *Am J Sports Med*. 2013;41(7):1674-1683.
- Cohen J. A coefficient of agreement for nominal scales. *Educ Psychol Meas*. 1960;20(1):37-46.
- Denard PJ, Brady PC, Adams CR, Tokish JM, Burkhart SS. Preliminary results of arthroscopic superior capsule reconstruction with dermal allograft. *Arthroscopy*. 2018;34(1):93-99.
- Duralde XA, Bair B. Massive rotator cuff tears: the result of partial rotator cuff repair. *J Shoulder Elbow Surg*. 2005;14(2):121-127.
- Fuchs B, Weishaupt D, Zanetti M, Hodler J, Gerber C. Fatty degeneration of the muscles of the rotator cuff: assessment by computed tomography versus magnetic resonance imaging. *J Shoulder Elbow Surg*. 1999;8(6):599-605.
- Gerber C, Maquieira G, Espinosa N. Latissimus dorsi transfer for the treatment of irreparable rotator cuff tears. *J Bone Joint Surg Am*. 2006;88(1):113-120.
- Gong H, Huang B, Zheng Z, Fu L, Chen L. Clinical use of platelet-rich plasma to promote tendon-bone healing and graft maturation in anterior cruciate ligament reconstruction - a randomized controlled study. *Indian J Orthop*. 2022;56(5):805-811.
- Goutallier D, Postel JM, Bernageau J, Lavau L, Voisin MC. Fatty muscle degeneration in cuff ruptures: pre- and postoperative evaluation by CT scan. *Clin Orthop Relat Res*. 1994;304:78-83.
- Gupta PK, Acharya A, Khanna V, Mourya A. Intra-femoral tunnel graft lengths less than 20 mm do not predispose to early graft failure, inferior outcomes or poor function. A prospective clinico-radiological comparative study. *Musculoskelet Surg*. 2023;107(2):179-186.
- Hamada K, Fukuda H, Mikasa M, Kobayashi Y. Roentgenographic findings in massive rotator cuff tears. A long-term observation. *Clin Orthop Relat Res*. 1990;254:92-96.
- Hughes JD, Davis B, Whicker E, et al. Nonarthroplasty options for massive, irreparable rotator cuff tears have improvement in range of motion and patient-reported outcomes at short-term follow-up: a systematic review. *Knee surgery, sports traumatology, arthroscopy: official journal of the ESSKA*. 2023;31(5):1883-1902.
- Ishihara Y, Mihata T, Tamboli M, et al. Role of the superior shoulder capsule in passive stability of the glenohumeral joint. *J Shoulder Elbow Surg*. 2014;23(5):642-648.
- Kholinne E, Kwak JM, Cho CH, et al. Arthroscopic superior capsular reconstruction for older patients with irreparable rotator cuff tears: a comparative study with younger patients. *Am J Sports Med*. 2021;49(10):2751-2759.
- Kholinne E, Kwak JM, Kim H, Koh KH, Jeon IH. Arthroscopic superior capsular reconstruction with mesh augmentation for the treatment of irreparable rotator cuff tears: a comparative study of surgical outcomes. *Am J Sports Med*. 2020;48(13):3328-3338.
- Kim DM, Shin MJ, Kim H, et al. Comparison between autografts and allografts in superior capsular reconstruction: a systematic review of outcomes. *Orthop J Sports Med*. 2020;8(3):2325967120904937.
- Landis JR, Koch GG. The measurement of observer agreement for categorical data. *Biometrics*. 1977;33(1):159-174.
- Lee JB, Kholinne E, Yeom JW, et al. Effect of fatty infiltration of the infraspinatus muscle on outcomes and graft failure after arthroscopic superior capsule reconstruction for irreparable posterosuperior rotator cuff tears. *Am J Sports Med*. 2022;50(14):3907-3914.
- Lim S, AlRamadhan H, Kwak JM, Hong H, Jeon IH. Graft tears after arthroscopic superior capsule reconstruction (ASCR): pattern of failure and its correlation with clinical outcome. *Arch Orthop Trauma Surg*. 2019;139(2):231-239.
- Lin J, Sun Y, Chen Q, et al. Outcome comparison of graft bridging and superior capsule reconstruction for large to massive rotator cuff tears: a systematic review. *Am J Sports Med*. 2020;48(11):2828-2838.
- Lin R, Zhong Q, Wu X, et al. Randomized controlled trial of all-inside and standard single-bundle anterior cruciate ligament reconstruction with functional, MRI-based graft maturity and patient-reported outcome measures. *BMC Musculoskelet Disord*. 2022;23(1):289.
- Macaulay AA, Greiwe RM, Bigliani LU. Rotator cuff deficient arthritis of the glenohumeral joint. *Clin Orthop Surg*. 2010;2(4):196-202.
- Malavolta EA, Assunção JH, Ramos FF, et al. Serial structural MRI evaluation of arthroscopy rotator cuff repair: does Sugaya's classification correlate with the postoperative clinical outcomes? *Arch Orthop Trauma Surg*. 2016;136(6):791-797.
- Mihata T, Lee TQ, Hasegawa A, et al. Five-year follow-up of arthroscopic superior capsule reconstruction for irreparable rotator cuff tears. *J Bone Joint Surg Am*. 2019;101(21):1921-1930.
- Mihata T, Lee TQ, Hasegawa A, et al. Arthroscopic superior capsule reconstruction can eliminate pseudoparalysis in patients with irreparable rotator cuff tears. *Am J Sports Med*. 2018;46(11):2707-2716.
- Mihata T, Lee TQ, Watanabe C, et al. Clinical results of arthroscopic superior capsule reconstruction for irreparable rotator cuff tears. *Arthroscopy*. 2013;29(3):459-470.
- Mihata T, McGarry MH, Kahn T, et al. Biomechanical effects of acromioplasty on superior capsule reconstruction for irreparable supraspinatus tendon tears. *Am J Sports Med*. 2016;44(1):191-197.
- Mihata T, McGarry MH, Pirolo JM, Kinoshita M, Lee TQ. Superior capsule reconstruction to restore superior stability in irreparable rotator cuff tears: a biomechanical cadaveric study. *Am J Sports Med*. 2012;40(10):2248-2255.
- Mirzayan R, Acevedo DC, Sidell MA, et al. Classification system of graft tears following superior capsule reconstruction. *Clin Imaging*. 2022;83:11-15.
- Neer CS 2nd, Craig EV, Fukuda H. Cuff-tear arthropathy. *J Bone Joint Surg Am*. 1983;65(9):1232-1244.
- Niglis L, Collin P, Dosch JC, Meyer N, Kempf JF. Intra- and inter-observer agreement in MRI assessment of rotator cuff healing using the Sugaya classification 10years after surgery. *Orthop Traumatol Surg Res*. 2017;103(6):835-839.
- Patte D. Classification of rotator cuff lesions. *Clin Orthop Relat Res*. 1990;254:81-86.
- Saito M, Morikawa T, Iwasaki J, et al. Influence of age on signal intensity of magnetic resonance imaging and clinical outcomes in double-bundle anterior cruciate ligament reconstruction: comparisons among different age groups. *Am J Sports Med*. 2022;50(1):93-102.
- Schiefer M, Mendonça R, Magnanini MM, et al. Intraobserver and interobserver agreement of Goutallier classification applied to magnetic resonance images. *J Shoulder Elbow Surg*. 2015;24(8):1314-1321.
- Sugaya H, Maeda K, Matsuki K, Moriishi J. Functional and structural outcome after arthroscopic full-thickness rotator cuff repair: single-row versus dual-row fixation. *Arthroscopy*. 2005;21(11):1307-1316.



37. Tran EP, Dingel AB, Terhune EB, et al. Anterior cruciate ligament length in pediatric populations: an MRI study. *Orthop J Sports Med.* 2021;9(4):23259671211002286.
38. van Groningen B, van der Steen MC, Janssen DM, et al. Assessment of graft maturity after anterior cruciate ligament reconstruction using autografts: a systematic review of biopsy and magnetic resonance imaging studies. *Arthrosc Sports Med Rehabil.* 2020;2(4):e377-e388.
39. Werthel JD, Vigan M, Schoch B, et al. Superior capsular reconstruction - a systematic review and meta-analysis. *Orthop Traumatol Surg Res.* 2021;107(8S):103072.
40. Woodmass JM, Wagner ER, Borque KA, et al. Superior capsule reconstruction using dermal allograft: early outcomes and survival. *J Shoulder Elbow Surg.* 2019;28(6S):S100-S109.
41. Yoshida M, Collin P, Josseaume T, et al. Post-operative rotator cuff integrity, based on Sugaya's classification, can reflect abduction muscle strength of the shoulder. *Knee Surg Sports Traumatol Arthrosc.* 2018;26(1):161-168.
42. Zachurzok A, Mayr J, Rutz E, Tomaszewski R. Dimensions of the anterior cruciate ligament and thickness of the distal femoral growth plate in children: a MRI-based study. *Arch Orthop Trauma Surg.* 2023; 143(5):2363-2372.
43. Zhang J, Ma J, Huang J, et al. Feasibility study of early prediction of postoperative MRI findings for knee stability after anterior cruciate ligament reconstruction. *BMC Musculoskelet Disord.* 2021; 22(1):649.